HHS Public Access

Author manuscript

Pain. Author manuscript; available in PMC 2018 August 01.

Published in final edited form as:

Pain. 2017 August ; 158(8): 1586–1598. doi:10.1097/j.pain.0000000000000961.

Repeated exposure to sucrose for procedural pain in mouse pups leads to long-term widespread brain alterations

Sophie Tremblay[1,2,3], **Manon Ranger**[1,2,4], **Cecil MY Chau**[1,2], **Jacob Ellegood**[5], **Jason P. Lerch**[5,6], **Liisa Holsti**[2,7], **Daniel Goldowitz**[2,3], and **Ruth E. Grunau**[1,2,*]

[1]Pediatrics, University of British Columbia, Vancouver, BC, Canada

[2]B.C. Children's Hospital Research Institute, Vancouver, BC, Canada

[3]Centre for Molecular Medicine and Therapeutics, Vancouver, BC, Canada

[4]Psychiatry, Developmental Neuroscience Division, & Nurture Science Program, Columbia University, New York, NY, USA

[5]Mouse Imaging Centre, Hospital for Sick Children, Toronto, ONT, Canada

[6]Medical Biophysics, University of Toronto, Toronto, ONT, Canada

[7]Occupational Science & Occupational Therapy, University of British Columbia, Vancouver, BC, Canada

1.0 Introduction

Infants born very preterm (≤32 weeks gestational age) spend weeks to months in neonatal intensive care units (NICU), undergoing on average 10 painful procedures per day [54] while their brains are rapidly developing. In rodents, early pain exposure has adverse effects on brain development [2,27,39] and social behaviors [1,11]. Clinical human prospective longitudinal cohort studies have demonstrated adverse effects of repetitive exposure to early pain on brain development and outcomes [16,25,48,49,67,70].

Effective pain management is crucial to help mitigate these negative consequences of early pain exposure. Currently, oral sucrose is administered routinely to reduce pain of minor procedures in infants and is recommended as standard care in international guidelines [4,5,43], which are based on evidence of safety and efficacy of a single dose of sucrose to reduce pain behaviors [62]. Importantly, long-term benefits or risks of repeated sucrose administration in the context of pain, in human or animal neonates, on brain development have not been studied. To date, one study in very preterm infants showed that more than 10 sucrose doses per day in the first week of life was associated with poorer attention and motor function, but the end-point was only at term-equivalent age [38]. Since oral sucrose is advocated as standard care worldwide [4,5,43], clinical equipoise no longer exists for a randomized controlled trial of sucrose in infants to evaluate effects on brain development.

*Corresponding author. rgrunau@bcchr.ca (R.E.G).

Mechanisms of sucrose-induced analgesia are well established in rodent models. Oral administration of sweet substances, such as sucrose, inhibit pain by mediating endogenous opioid peptide and μ1-opioid receptor actions [21]. Others have suggested additional involvement of the 5-HT2A-serotonergic receptors in the antinociception effect of sweet solution administration[51]. Additionally, key brainstem sites critically involved in descending pain modulation (e.g. periaqueductal gray and rostroventromedial medullary region) have been shown to be activated by intraoral sucrose administration in rat pups [6]. One study has reported short-term memory impairment in rats repeadly exposed during the first 8 weeks of life to daily pain alone compared to pain combined with sucrose[45]. However, their pain model does not match that of the human infant exposure in the NICU.

Sugar consumption activates common reward pathways and repeated sugar exposure is known to cause excessive dopamine and acetylcholine release, as well as opioid stimulation [32,34,47,59]. In the developing brain, it is not known whether increases in dopamine and/or acetylcholine levels, as well as opioid stimulation would have positive or negative effect on related brain structures and functions [35].

Given that sucrose administration for procedural pain is a treatment that currently affects many thousands of preterm infants annually, it is crucial to determine the long-term benefits/risks of repetitive sucrose. In the present study we examined effects of neonatal repetitive sucrose treatment on brain development in a mouse pain model and amount of oral sucrose exposure that closely mimics NICU care.

2.0 Materials and methods

2.1. Animals

Mice make an excellent preclinical model to study conditions in the human preterm neonate because they are born neurologically immature, with the first postnatal week in the mouse corresponding to the development of the human limbic system, striatum and cerebellar development at 24 to 32 weeks gestation [12]. All procedures were approved by the University of British Columbia Animal Care Committee and conform to the guidelines of the Canadian Council on Animal Care. C57BL/6J mice used in this study were obtained from the Goldowitz mouse colony at the Center for Molecular Medicine and Therapeutics Animal Facility. Animals were maintained on a 14/10 hour light/dark cycle with food and water *ad libitum*. All mice were provided with nestlets and Plexiglas igloo-style houses as part of standard enrichment. A specific cellulose bedding was used during the entire protocol duration to minimize stimulation and discomfort of inflamed paws in the pups (¼ inch pelleted cellulose, Biofresh, USA). Multiparous female mice were individually mated with a male stud. Pregnant females were group housed until E17, upon which they were divided and housed with a nulliparous female CD-1 used as a “nanny” to improve survival and reduce cannibalism of mouse pups. This housing was maintained for the duration of pregnancy and lactation. The day of birth was considered P0. Pups were kept with their mother until wean age, postnatal day 21 (P21). After weaning, mice were housed together with appropriate nesting materials, enrichment and cellulose bedding (5 mice/cage, sex-matched cages) during aging until P85–P95.

2.2. Needle-prick model combined with oral sucrose

Newborn mouse pups on P0 were randomized to one of the six groups and tattooed on their paw using a single 30G needle prick to allow individual identification. Pups received either sterile water or sucrose (Vehicle; Treatment) given orally by a micropipette 2 minutes prior to one of the three interventions: paw needle-prick, light paw tactile pressure with a cotton-tipped swab, or only being handled in a similar manner to other intervention groups. Treatment/Intervention sequence duration was less than 5 minutes per interval. A solution of sucrose 24% w/v (Sucrose ≥99.5% (GC), Sigma, USA, cat#S7903) in sterile water, filtered with 0.22μm filter, or sterile water was used intraorally as analgesic treatment 2 minutes before the intervention. Using a micropipette and sterile tips, the treatment was administered either on the anterior part of the tongue or inner-cheek of the mouth. An equivalent dose of sucrose per weight comparable to the recommended dose for human neonates was given. The standard guideline recommends 0.5mL per dose for very preterm infants (24 to 32 weeks of gestation), which correspond to 0.08g–0.2g of sucrose per body weight (kg) [62]. Each pup received 0.1–0.2g of sucrose per kg of mouse body weight. Each dose was adjusted daily based on the mouse pup weight. Vehicle treatment group received orally an equivalent volume of sterile water. Treatment/Intervention was administered 10 times per day per mouse pup over a 10-hour period (from 8AM until 6PM) during the day (light) cycle from P1 to P6 inclusive. Each treatment/intervention was spaced by a minimum of 30 minutes to allow enough time for feeding and recovery from the interventions. Forepaws and hindpaws were alternated over each intervention and only one paw was touched or pricked during each interval. Needle-pricks were performed using a 30G sterile needle (0.3mm outer diameter) angled at 10–15 degrees from the skin to carefully pierce only the surface of the skin. Penetration of deeper layers, such as tendon or bone, was avoided. Mouse pups were returned to the dams between each hourly Treatment/Intervention sequences. During the procedure, home cages with nursing females were placed in a separate room to decrease their stress in response to mouse pup vocalizations related to the interventions. Each procedure was performed on a warmed heating pad to avoid any heat loss. At P7, mice pups remained in their home cage with their dam until weaning (P21). A total of 109 mouse pups were treated and survived to adulthood with an overall survival rate of 88%.

2.3. Perfusion and tissue collection

Adult brains were collected between P85–P95 for MRI scanning. Initially the mice were anesthetized and transcardially perfused with 10mL of 0.1M PBS containing 10U/mL heparin (PPC, CA, cat#C504805) and 2mM ProHance (a Gadolinium contrast agent, Bracco Diagnostics, USA, cat#111181) followed by 10mL of 4% paraformaldehyde (PFA) (Cedarlane, CA, cat#15710) in 0.1M PBS containing 2mM ProHance [60]. Perfusions were performed at a rate of approximately 60mL/hr. After perfusion, mice were decapitated. The brain and remaining skull structures were incubated in 4% PFA + 2mM ProHance overnight at 4°C then transferred to 0.1M PBS containing 2mM ProHance and 0.02% sodium azide for at least seven days prior to MRI scanning.

2.4. Magnetic resonance imaging, registration and analysis

A multi-channel 7.0 Tesla MRI scanner (Varian Inc., Palo Alto, CA) was used to image the brains within skulls. Sixteen custom-built solenoid coils were used to image the brains in parallel [15]. T2-weighted, three-dimensional fast spin echo sequence, with a cylindrical acquisition of k-space, and with repetition time TR = 350 ms, echo train length = 6, TE_{eff} = 12 ms, field of view (FOV) 20mm×20mm×25mm^3, and matrix size of 504 × 504 × 630, which provided an isotropic resolution of 0.04 mm were used to gather anatomical imaging and volume change parameters. Total imaging time was ~14 hours.

To visualize and compare any changes in the mouse brains, images were linearly (6 parameter followed by a 12 parameter) and non-linearly registered against a pre-existing atlas [26]. All scans were then re-sampled with the appropriate transformation and averaged to create a population atlas representing the average anatomy of the study sample. The resulting registration was to have all scans deformed into alignment with each other in an unbiased fashion. This strategy allowed for the analysis of the deformations needed to take each individual mouse's anatomy into this final atlas space, the goal being to model how the deformation fields relate to treatment/intervention [42,44]. The Jacobian determinants of the deformation fields were calculated as measures of volume at each voxel. Significant volume changes were calculated by warping a pre-existing classified MRI atlas onto the population atlas, which allowed assessment of the volumes of 159 segmented structures encompassing cortical lobes, large white matter structures (i.e. corpus callosum), ventricles, cerebellum, brain stem, and olfactory bulbs in all brains [26]. The current atlas used is a combination of three atlas segmentations: A 62 region full brain segmentation [26], and additional segmentation of the cortex [66] and cerebellum [61,66]. This 159 region atlas was used to assess regional differences across the brain. Further, these measurements were examined on a voxel-wise basis to localize the differences found within regions or across the brain.

2.5. Statistical analysis

We first conducted multiple one-sided ANOVAs to determine whether there was any effect by intervention (Handle, Tactile, or Needle-prick), treatment (Vehicle or Sucrose), or an intervention by treatment interaction for each of the 159 regional brain volumes. Multiple comparisons were controlled for using the False Discovery Rate (FDR) [30].

Constrained principal component analysis (CPCA) was used to examine the group differences of effects of needle-prick and sucrose exposure upon all 159 regional brain volumes. CPCA is a 2-step process, referred to as the external and internal analysis. The external analysis consists of a multivariate least squares multiple regression of the dependent measures on the independent measures, producing predicted and residual scores for each dependent measure [48,49]. The internal analysis is a principal component analysis (PCA), which transforms aforementioned regression matrices into a few orthogonal components (or latency variables) which explain the maximum amount of variance.

CPCA captures the most prominent feature in a data matrix and projects it to a subspace of minimal dimensionality according to the external information [64]. The lowest dimension, which explains the greatest variation, depends on both the dataset and the external

information. Since the aim of the study was to investigate the effects of sucrose on the interventions, three CPCA models were built to capture the contrasts between groups. The first CPCA was to compare regional brain volumes between Vehicle and Sucrose treatment groups. Second and third CPCA models were built to compare the effect of Treatment exposure within the Vehicle and Sucrose treatment group respectively.

In the first CPCA, the independent variables matrix of the external analysis included Vehicle treatment group and Sucrose treatment group, sex, and the adjusted total brain volume. The adjusted total brain volumes were computed as the residuals of regressing total brain volumes onto Vehicle/Sucrose groups and intervention groups. The purpose was to remove the possible association between sucrose and needle-prick exposure and the total brain volume. Two separate CPCAs were then performed by splitting the sample into Vehicle treated and Sucrose treated mice. The independent variable matrix of each CPCA included Intervention (i.e. Handle vs Tactile, Handle vs Needle-prick), sex, and adjusted total brain volume.

The internal analysis consists of PCAs on each of the aforementioned matrices. The resulting component solutions (overall, predicted, and residual solutions) are examined to determine which dimensions of the regional brain volumes can be explained by the independent variables. Details of CPCA have been described previously [19,48,49]. Computations for CPCA were done using MATLAB v 7.11 (The MathWorks, 2010, Natick, Massachusetts). Multiple comparisons were corrected by Bonferroni method. Data were graphically organized using GraphPad Prism (San Diego, CA).

3.0 Results

3.1. Repeated sucrose pain model details

At P0, mouse pups (50 males; 59 females) were randomly allocated to one of six groups: Vehicle/Handle ($n = 18$), Vehicle/Tactile ($n = 16$), Vehicle/Needle-prick ($n = 18$), Sucrose/Handle ($n = 17$), Sucrose/Tactile ($n = 22$), or Sucrose/Needle-prick ($n = 18$) (Figure 1C). Each litter included at least two different groups and nearly equal distribution by sex per group. During the first days of life, from postnatal day 1 to 3 (P1 to P3), pups in the needle-prick groups showed visible paw inflammation at the site of skin-break as exposure to the intervention accumulated throughout the 10 hours (Figure 1A); in each case, local inflammation disappeared by the following morning. No signs of infection or other complications occurred. Timeline of the experimental design is shown in Figure 1B.

Over the treatment period (P1–P7), suckling behavior was not affected by sucrose exposure reflected by non-significant changes in mean weight gain over the treatment period between groups ($F_{5,103} = 2.050$, $P = 0.0778$) (Figure 1C). Similar weight gain across groups persisted beyond the treatment period up to weaning ($F_{5,102} = 1.639$, $P = 0.1564$). Likewise, there was no significant difference in mean body weight between groups at scanning time ($F_{5,103} = 0.350$, $P = 0.8815$).

3.2. Early repetitive sucrose exposure leads to widespread smaller regional brain volumes

To explore the effects of P1 to P6 repeated exposure to sucrose on long-term brain development, we initially examined volumes of 159 independent brain regions in adult mice that either received Vehicle ($n = 52$) or Sucrose ($n = 57$) treatment before the intervention (either Handle, Tactile, or Needle-prick). Overall, we found significant differences in multiple regions with respect to treatment, with 21 out of 159 regions being significantly smaller in mice exposed to sucrose ($P < 0.0001$; false discovery rate [FDR] < 5%) (Figure 2A). White matter structures were particularly affected by sucrose treatment. For example, compared to the Vehicle groups, smaller volumes were found in the Sucrose groups for the corpus callosum ($P < 0.0001$; FDR = 3%) and fimbria ($P < 0.0001$; FDR = 1%). Only trends were seen when examining the effects of intervention only and treatment-intervention interaction; no significant sex differences were found. Figure 2A lists the results of the significant one-way ANOVAs ($P < 0.0001$, FDR < 5% to $P < 0.03$, FDR < 15%) for each brain region. We further explored the effect of sucrose exposure on brain volumes by grouping 159 brain regions into seven major divisions (cortex, cerebellum, ventricles, brainstem, olfactory region, grey and white matter) to limit the number of examined regions. Here, we found that adult mice exposed to sucrose as pups had significantly smaller volumes in the white matter, cerebellum and ventricles ($P < 0.0001$; FDR < 5%) (Figure 2B). Trends were observed in cerebral grey matter ($P = 0.003$; FDR = 6%). As before, we did not find any significant effects of intervention only, treatment-intervention interaction, or sex.

Figures 2C and 2D provide box-plot examples of significant and non-significant volume differences found in specific brain regions. A complete list of brain mean volumes for the 159 regions measured is provided in supplementary material (Table S1 and Table S2) along with group comparisons for effect of Treatment (Vehicle vs Sucrose) or Intervention (Needle-prick [pain] vs all other interventions).

3.3. Constrained principal component analysis confirms Sucrose treatment damaging effect on brain volumes

To confirm and further explore the effect of exposure to treatment and intervention found using ANOVA, we used constrained principal component analysis (CPCA) [64] to examine the component structure of the variance in the brain volumes that is specifically predicted by a set of predictor variables: total brain volume, sex and study groups. CPCA allowed us to conduct a multiple regression analysis of the regional brain volumes in relation to the treatment group, sex and total brain volume, and then condense the results into components. Hence, in the present study, the matrix of predicted component scores reflected the variance in regional brain volumes that was accounted for by total brain volume, sex and study groups.

First we examined the 159 regional volumes in relation to treatment (i.e. Vehicle vs Sucrose), irrespective of intervention. The external analysis of CPCA (see Methods section for further details) showed that the three predictors included in our model (total brain volume, sex, and treatment) accounted for 49% of the overall variance in regional brain volume (Table 1). Two main principal components (PC) were extracted from the predicted solution, explaining respectively 26.2% and 22.7% of the variance in brain volumes of the

159 regions examined. Based on the distribution of predictors on each principal component, we interpreted PC1 as representing total brain volume and sex effects, and PC2 as representing treatment effects. Predictor variables with positive loadings were associated with larger regional brain volumes. Total brain volume positively loaded on both components, which indicated larger total brain volume was associated with larger regional volumes, whereas in contrast, the negative loading for treatment indicates smaller brain volumes was associated with sucrose exposure. Treatment (reflected in PC2) uniquely loaded on 22 out of the 159 brain regions largely comprising of cerebellar grey and white matter, showing smaller volumes in cortical amygdaloid, hippocampus, stria terminalis and hypothalamus; indicating that mice exposed to sucrose had smaller volumes in those areas compared to those exposed to vehicle (Table 2).

3.3.1 Needle-prick intervention has no effect on brain volumes—To examine the effects of treatment (Vehicle, Sucrose) within the three intervention groups (Handle, Tactile, and Needle-prick), two distinct CPCAs were conducted by splitting the sample by treatment group assignment, i.e. Vehicle versus Sucrose. To examine effects of Tactile and Needle-prick intervention, Handle was used as the reference intervention, i.e. Tactile vs Handle, Needle-prick vs Handle in each analysis.

When examining the effect of the interventions in mice exposed to **vehicle**, our CPCA showed that the four predictors included in our model (total brain volume, sex, Needle-prick intervention, and Tactile intervention) accounted for 44% of the overall variance in regional brain volumes. Three principal components (PC) were extracted from the predicted solution where PC1 reflected total brain volume and sex, PC2 reflected Tactile intervention, and PC3 reflected sex and Tactile intervention, explaining respectively 22%, 15.3%, and 6.3% of the variance in brain volumes of the 159 regions examined (Table 3). Predictor variables with positive loadings were associated with larger regional brain volumes. The Needle-prick intervention predictor did not load significantly on any PC, indicating that regional brain volumes were not different between the Vehicle/Needle-prick and Vehicle/Handle groups. Thus, mice repeatedly exposed to needle-pricks did not have significantly different regional brain volumes from those that were just handled. Tactile intervention positively loaded on PC2 and negatively on PC3, which indicated that Tactile intervention was not associated with those brain regions loaded on both components. Accordingly, Tactile intervention (reflected here in PC2) was solely related to volumes in 40 brain regions out of the 159 brain regions that were examined (Table 4; Bonferroni cut-off for significance [$P < 0.013$]). Therefore, mice in the Vehicle/Tactile group compared to Vehicle/Handle had bigger volumes in those structures, such as the hippocampus, midbrain, nucleus accumbens, and cerebellar subregions.

3.3.2. Smallest brain volumes found in mice given sucrose treatment before needle-prick intervention—The CPCA for the Sucrose treatment showed that the four predictors included in our model (total brain volume, sex, Needle-prick intervention, and Tactile intervention) accounted for 55% of the overall variance in regional brain volumes. Three principal components (PC) were extracted from the predicted solution, where PC1 reflected Needle-prick and Tactile interventions, PC2 total brain volume and sex, and PC3

reflected all four predictors, explaining respectively 33.6%, 17.3%, and 4.3% of the variance in brain volumes of the 159 regions examined (Table 5). Predictor variables with positive loadings were associated with larger regional brain volumes. Dominant loadings on PC1 were widespread, with highly significant loadings in 95 brain regions (Table 6; Bonferroni cut-off for significance [$P < 0.013$]). Given that in PC1 the predictor loading for Needle-prick was negative and that the loading for Tactile was positive (loadings −0.469 and 0.428 respectively; see Table 5), this indicated that mice in the Sucrose/Needle-prick group compared to Sucrose/Handle group had smaller volumes in those structures with significant loadings on PC1, whereas mice in the Sucrose/Tactile group compared to Sucrose/Handle had bigger volumes in structures with significant loadings on PC1. These regions included the amygdala, cerebellum, primary and secondary somatosensory cortices, thalamus, hippocampus, cingulate cortex, and periaqueductal grey.

4.0 Discussion

Using a neonatal mouse model that closely mimics NICU procedural pain and treatment, we found widespread long-term alterations in adult white and grey matter brain volumes in mouse pups repeatedly exposed to sucrose in the first week of life, which approximates the preterm period in humans. Repetitive sucrose exposure induced smaller brain volumes mainly in white matter regions of the forebrain, cerebellum, and hippocampus. To our knowledge, this is the first animal or human study to examine long-term effects on brain of neonatal repetitive sucrose exposure for pain treatment relevant to NICU care. Whereas, Nuseir et al. [45] exposed newborn rats to daily repetitive pain and/or sucrose over a prolonged period of 8 weeks, which is exposure lasting far beyond the neonatal period, we used a pain model that matches that of the human infant exposure in the NICU. Importantly, we found deleterious effects of early sucrose treatment irrespective whether mouse pups were handled, touched or needle-pricked at the time sucrose was administered. Our findings raise serious questions relating to the current widespread use of sucrose for procedural pain management in NICUs worldwide. Of even greater concern, is that when analyzing the data by splitting the sample by intervention exposure (i.e. Vehicle versus Sucrose), we found that from all the pups that were exposed to sucrose prior to a treatment (i.e. handling, touch, needle-prick), it was the ones that received needle-pricks that had the worst outcome. This particular group of mice had smaller regional brain volumes predominately in areas involved in nociceptive processing (e.g. primary somatosensory cortices, thalamus, cingulate cortex, periaqueductal grey); whereas, this effect was not observed in mice that received water. This suggests that sucrose is not providing brain-protection and may even have an opposite effect on brain especially when given in combination with pain.

Sucrose is widely accepted as an effective nonpharmacological intervention for pain of minor procedures in preterm infants [29,62]. Exposure to single sucrose treatment is safe and spared of serious short-term side effects. However, one study has shown poorer neurological development around term equivalent age in preterm infants exposed to more than 10 doses of sucrose per 24h in the first week of life [38] and our results of reduced brain volume are consistent with these findings. There are increasing concerns regarding the limited evidence of long-term safety of repeated exposure to sucrose for procedural pain management in the preterm population [20].

The rewarding effects of ingesting sweet solutions, such as sucrose, a disaccharide combination of glucose and fructose, appear to be mediated by similar neuronal pathways and mechanisms implicated in drug abuse. Indeed, sucrose has opioid-like effects on dopamine receptors comparable to morphine [59]. Thus, the deleterious effect of sucrose on brain volumes after repeated administration seen in this study may be explained through the mechanism underlying sucrose's mitigating effect on pain. Opioid-induced neurotoxicity has been largely explored in preclinical studies showing reduced neuronal density and dendritic length, as well as induced neuronal apoptosis in rodent pups exposed to morphine [8,33,53,57]. Early opioid exposure also induces apoptosis of fetal microglia and neurons in vitro [36] and compromises myelination [56]. Accordingly, these apoptotic and anti-proliferative effects described could also occur after sucrose exposure in the developing brain and could explain, at least partially, the widespread effect on brain regions we observed.

There are concerns currently about possible effects of pre-emptive morphine infusions in ventilated preterm infants, particularly at higher doses, based on findings from randomized control trials (RCTs) [3,50,58], leading to recommendations of judicious use in this population [10]. Follow-up studies of long-term neurodevelomental outcomes have reported mixed findings [22,23,28]. A single-site longitudinal cohort study of very preterm children showed an independent association between neonatal exposure to morphine and impaired cerebellar growth in the neonatal period (in a dose-dependent manner) [71]. Our current findings with early exposure to sucrose appear to be consistent with clinical and preclinical findings of opioid exposure, such that repetitive sucrose administration had adverse effects that were seen mainly in hippocampal areas and cerebellar lobules.

Importantly, Asmerom *et al.* [7] found that after a single dose of sucrose before a heel lance, preterm neonates had tachycardia, higher oxidative stress and adenosine triphosphate (ATP) breakdown. Given that multiple doses of sucrose are administered daily to preterm infants [18], the pathophysiological mechanisms involved in this recurrent sucrose-induced oxidative stress exposure may partially explain the widespread alterations of white matter tracts seen in our study. Indeed, excitotoxicity and oxidative stress are known as factors involved in maturation of pre-oligodendrocytes (pre-OLC) and oligodendrocytes (OLC) in premature brain white matter injury [9] leading to delayed or arrested OLC development [17] and delayed myelination [37]. In rodents, these cells proliferate, migrate and differentiate during the first two postnatal weeks, whereas in humans they develop predominantly in the second half of pregnancy [55]. Here, we found that repetitive sucrose during the first postnatal week in mice resulted in smaller cerebellar white matter volume and forebrain fiber tracts suggestive of a deleterious sucrose effect on OLC maturation and myelination.

Unique to our model is the administration of minute quantities of sucrose absorbed prominently through the oral mucosa, mimicking the standardized non-pharmacological pain treatment use of sucrose in NICU care worldwide. Absorption, metabolism and differing brain activation pathways must be taken into account when comparing our results to findings from models of sugar binge eating where sucrose solutions are being infused directly into the rodents' stomach or animals feed ad libidum sucrose solutions/high caloric diets. Indeed,

binge sugar intake has opioid-like effects and activates the reward system through the nucleus accumbens and the adjacent caudate-putamen [59], whereas repetitive exposure to small quantities of oral sucrose may activate different neurological pathways. Based on our findings that sucrose exposure induced altered regional brain volumes prominently in large afferent white matter tracts implicated in the hypothalamic–pituitary–adrenal (HPA) axis/stress system (e.g. fimbria, stria terminalis), and that we did not find significant volume alterations in the nucleus accumbens, we question which pathway is predominantly affected by early repetitive exposure to sucrose in this context. Evidence in rodents has shown the effects of sucrose/carbohydrates on regulation of the HPA axis [68]. Moreover, results of rodent studies have suggested that sweet solutions modulate pain through opioid mechanisms [13,40,52]. The evidence is less clear in human infants with few studies having examined potential mechanisms of action of sucrose [14,31,63] and results suggest that mechanisms other than those mediated by opioid pathways may be involved in the effects of sucrose [35]. Further studies are needed.

Surprisingly, we did not find a significant long-term effect of early repetitive *pain* exposure from needle-pricks on adult regional brain volumes, nor did we find a treatment-intervention interaction. According to previous studies in rodent pups, neonatal pain exposure (i.e. inflammatory pain from formalin injections or repetitive saline injections) was shown to modify both the structure and function of the developing brain [2,27,39]. Thus, we were expecting that mice exposed to needle-pricks during the first week of life would have altered brain development, which was not the case. Methodological differences may account for these findings, inflammatory pain or pain from injections may not have the same consequences as needle-pricks. We question the invasiveness of our needle-prick pain stimulus, given that we used very thin needles (30G) and did not penetrate deeper layers, such as tendon or bone, in contrast to the apparently more invasive procedures used in needle-prick pain in previous rat studies [1,27,41]. It should be noted that we undertook interventions 10 times daily for six days, based on the median exposure to painful procedures during NICU care [54].

Importantly, distinctive to our study was the addition of a CD-1 female mouse as a “nanny” to support the mother and improve survival of mouse pups, which could have added a buffering effect on pain through increased grooming and nurturing. Maternal behavior (grooming and licking) has been shown to modulate effects of early pain exposure in rats [24,69], where increased maternal behaviors reduced inflammation in response to neonatal formalin injections during the first two weeks of life of rat pups and thermal sensitivity once in adulthood. This “nanny plus mother” model emphasizes the robustness of our current findings of permanently smaller regional brain volumes in relation to early repetitive sucrose exposure.

Some limitations to our study exist. At this time, we do not have histological data to support our brain volume findings, thus complete interpretation cannot be determined (e.g. apoptosis or decrease neuronal proliferation or changes in cortical blood volume or water content) [46,65]. Consequences of repetitive sucrose exposure on the developing brain should be further studied at the functional level to assess if long-term effects on brain induce differences in learning and behavior.

Currently, it is not possible to conduct randomized controlled clinical trials of sucrose for pain management in preterm neonates in the NICU, since sucrose is the standard of care. Therefore, our findings from a neonatal mouse model are critical, suggesting cautious use of repetitive sucrose administration in very preterm infants is warranted. Our work reinforces recent guidelines from the American Academy of Pediatrics [20] highlighting the lack of evidence on mechanisms of action and long-term consequences of repetitive oral sucrose use for procedural pain.

Split analysis by treatment (Sucrose) CPCA factor loadings for Sucrose groups model; three PCs were extracted from the predicted solution, where PC1 reflected Needle-prick intervention and Tactile intervention, PC2 total brain volume and sex, and PC3 reflected all four predictors; explained variance for PC1, PC2 and PC3 are 33.6%, 17.3%, and 4.3% respectively. Sucrose/Handle ($n = 17$), Sucrose/Tactile ($n = 22$), Sucrose/Needle-prick ($n = 18$). Significant loadings (Bonferroni $P < 0.013$) particular to intervention shown in **bold**.

Supplementary Material

Refer to Web version on PubMed Central for supplementary material.

Acknowledgments

We would like to thank the help of Hannah McNeill (visiting undergraduate student from the University of Nottingham, UK) and Zahra Ezzat-Zadeh during the experiments. S. Tremblay and M. Ranger contributed equally to the work; R.E. Grunau and D. Goldowitz share senior authorship equally.

Funding: This work was supported in part by the Eunice Kennedy Shriver Institute of Child Health and Human Development (NICHD/NIH) grant RO1 HD039783 (to REG), funds from the Canadian Child Health Clinician Scientist Program (to ST and MR) and NeuroDevNet. Dr. Grunau holds a Senior Scientist salary award from the BC Children's Hospital Research Institute; Fellowships support from the Canadian Institute of Health Research (CIHR) (to ST and MR), Pain In Child Health CIHR Strategic Training Initiative in Health (to MR), and Fonds Recherche Quebec-Santé (to ST and MR). We have no conflicts of interest to declare. Dr. Holsti is a lead inventor of a medical device for pain management for preterm infants. In partnership with the Provincial Health Services Association of British Columbia, Canada, she could, in the future, receive royalties as a result of licensing agreements made with private industry for commercialization of the device. She has not received any remuneration to date. In addition, she did not participate actively in the testing of the mice, or in the data analysis in this paper. None of the remaining authors have any affiliation, financial agreement, or other involvement that would place us in conflict of interest with this manuscript.

References

1. Anand KJ, Coskun V, Thrivikraman KV, Nemeroff CB, Plotsky PM. Long-term behavioral effects of repetitive pain in neonatal rat pups. Physiol Behav. 1999; 66:627–637. [PubMed: 10386907]
2. Anand KJ, Garg S, Rovnaghi CR, Narsinghani U, Bhutta AT, Hall RW. Ketamine reduces the cell death following inflammatory pain in newborn rat brain. Pediatr Res. 2007; 62:283–290. [PubMed: 17551412]
3. Anand KJ, Hall RW, Desai N, Shephard B, Bergqvist LL, Young TE, Boyle EM, Carbajal R, Bhutani VK, Moore MB, Kronsberg SS, Barton BA. NEOPAIN Trial Investigators Group. Effects of morphine analgesia in ventilated preterm neonates: primary outcomes from the NEOPAIN randomised trial. Lancet. 2004; 363:1673–1682. [PubMed: 15158628]
4. Anand KJ. International Evidence-based Group for Neonatal Pain. Consensus statement for the prevention and management of pain in the newborn. Arch Pediatr Adolesc Med. 2001; 155:173–180. [PubMed: 11177093]
5. Anand KJS, Bergqvist L, Hall W, Carbajal R. Acute Pain Management in Newborn Infants. Pain (Clinical Updates). 2011; 19:1–6.

6. Anseloni VC, Ren K, Dubner R, Ennis M. A brainstem substrate for analgesia elicited by intraoral sucrose. Neuroscience. 2005; 133:231–243. [PubMed: 15893646]

7. Asmerom Y, Slater L, Boskovic DS, Bahjri K, Holden MS, Phillips R, Deming D, Ashwal S, Fayard E, Angeles DM. Oral sucrose for heel lance increases adenosine triphosphate use and oxidative stress in preterm neonates. J Pediatr. 2013; 163:29–35. e1. [PubMed: 23415615]

8. Atici S, Cinel L, Cinel I, Doruk N, Aktekin M, Akca A, Camdeviren H, Oral U. Opioid neurotoxicity: comparison of morphine and tramadol in an experimental rat model. Int J Neurosci. 2004; 114:1001–1011. [PubMed: 15527204]

9. Back SA, Gan X, Li Y, Rosenberg PA, Volpe JJ. Maturation-dependent vulnerability of oligodendrocytes to oxidative stress-induced death caused by glutathione depletion. J Neurosci. 1998; 18:6241–6253. [PubMed: 9698317]

10. Bellu R, de Waal KA, Zanini R. Opioids for neonates receiving mechanical ventilation. Cochrane Database Syst Rev. 2008; (1):CD004212. [PubMed: 18254040]

11. Bhutta AT, Rovnaghi C, Simpson PM, Gossett JM, Scalzo FM, Anand KJ. Interactions of inflammatory pain and morphine in infant rats: long-term behavioral effects. Physiol Behav. 2001; 73:51–58. [PubMed: 11399294]

12. Biran V, Verney C, Ferriero DM. Perinatal cerebellar injury in human and animal models. Neurol Res Int. 2012; 2012:858929. [PubMed: 22530126]

13. Blass E, Fitzgerald E, Kehoe P. Interactions between sucrose, pain and isolation distress. Pharmacol Biochem Behav. 1987; 26:483–489. [PubMed: 3575365]

14. Blass EM, Ciaramitaro V. A new look at some old mechanisms in human newborns: taste and tactile determinants of state, affect, and action. Monogr Soc Res Child Dev. 1994; 59:I–V. 1–81. [PubMed: 8047076]

15. Bock NA, Nieman BJ, Bishop JB, Mark Henkelman R. In vivo multiple-mouse MRI at 7 Tesla. Magn Reson Med. 2005; 54:1311–1316. [PubMed: 16215960]

16. Brummelte S, Grunau RE, Chau V, Poskitt KJ, Brant R, Vinall J, Gover A, Synnes AR, Miller SP. Procedural pain and brain development in premature newborns. Ann Neurol. 2012; 71:385–396. [PubMed: 22374882]

17. Buser JR, Maire J, Riddle A, Gong X, Nguyen T, Nelson K, Luo NL, Ren J, Struve J, Sherman LS, Miller SP, Chau V, Hendson G, Ballabh P, Grafe MR, Back SA. Arrested preoligodendrocyte maturation contributes to myelination failure in premature infants. Ann Neurol. 2012; 71:93–109. [PubMed: 22275256]

18. Carbajal R, Rousset A, Danan C, Coquery S, Nolent P, Ducrocq S, Saizou C, Lapillonne A, Granier M, Durand P, Lenclen R, Coursol A, Hubert P, de Saint Blanquat L, Boelle PY, Annequin D, Cimerman P, Anand KJ, Breart G. Epidemiology and treatment of painful procedures in neonates in intensive care units. JAMA. 2008; 300:60–70. [PubMed: 18594041]

19. Chau CMY, Ranger M, Sulistyoningrum D, Devlin AM, Oberlander TF, Grunau RE. Neonatal pain and *COMT* Val158Met genotype in relation to serotonin transporter (*SLC6A4*) promoter methylation in very preterm children at school age. Front Behav Neurosci. 2014:8. [PubMed: 24478655]

20. Committee on Fetus and Newborn and Section on Anesthesiology and Pain Medicine. Prevention and Management of Procedural Pain in the Neonate: An Update. Pediatrics. 2016; 137:e20154271–4271. Epub 2016 Jan 25. [PubMed: 26810788]

21. de Freitas RL, Kubler JM, Elias-Filho DH, Coimbra NC. Antinociception induced by acute oral administration of sweet substance in young and adult rodents: the role of endogenous opioid peptides chemical mediators and mu(1)-opioid receptors. Pharmacol Biochem Behav. 2012; 101:265–270. [PubMed: 22197708]

22. de Graaf J, van Lingen RA, Simons SH, Anand KJ, Duivenvoorden HJ, Weisglas-Kuperus N, Roofthooft DW, Groot Jebbink LJ, Veenstra RR, Tibboel D, van Dijk M. Long-term effects of routine morphine infusion in mechanically ventilated neonates on children's functioning: five-year follow-up of a randomized controlled trial. Pain. 2011; 152:1391–1397. [PubMed: 21402444]

23. de Graaf J, van Lingen RA, Valkenburg AJ, Weisglas-Kuperus N, Groot Jebbink L, Wijnberg-Williams B, Anand KJ, Tibboel D, van Dijk M. Does neonatal morphine use affect

neuropsychological outcomes at 8 to 9 years of age? Pain. 2013; 154:449–458. [PubMed: 23352760]

24. de Medeiros CB, Fleming AS, Johnston CC, Walker CD. Artificial rearing of rat pups reveals the beneficial effects of mother care on neonatal inflammation and adult sensitivity to pain. Pediatr Res. 2009; 66:272–277. [PubMed: 19531973]
25. Doesburg SM, Chau CM, Cheung TP, Moiseev A, Ribary U, Herdman AT, Miller SP, Cepeda IL, Synnes A, Grunau RE. Neonatal pain-related stress, functional cortical activity and visual-perceptual abilities in school-age children born at extremely low gestational age. Pain. 2013; 154:1946–1952. [PubMed: 23711638]
26. Dorr AE, Lerch JP, Spring S, Kabani N, Henkelman RM. High resolution three-dimensional brain atlas using an average magnetic resonance image of 40 adult C57Bl/6J mice. Neuroimage. 2008; 42:60–69. [PubMed: 18502665]
27. Duhrsen L, Simons SH, Dzietko M, Genz K, Bendix I, Boos V, Sifringer M, Tibboel D, Felderhoff-Mueser U. Effects of repetitive exposure to pain and morphine treatment on the neonatal rat brain. Neonatology. 2013; 103:35–43. [PubMed: 23037996]
28. Ferguson SA, Ward WL, Paule MG, Hall RW, Anand KJ. A pilot study of preemptive morphine analgesia in preterm neonates: effects on head circumference, social behavior, and response latencies in early childhood. Neurotoxicol Teratol. 2012; 34:47–55. [PubMed: 22094261]
29. Gao H, Gao H, Xu G, Li M, Du S, Li F, Zhang H, Wang D. Efficacy and safety of repeated oral sucrose for repeated procedural pain in neonates: A systematic review. Int J Nurs Stud. 2016; 62:118–125. [PubMed: 27474944]
30. Genovese CR, Lazar NA, Nichols T. Thresholding of statistical maps in functional neuroimaging using the false discovery rate. Neuroimage. 2002; 15:870–878. [PubMed: 11906227]
31. Gradin M, Schollin J. The role of endogenous opioids in mediating pain reduction by orally administered glucose among newborns. Pediatrics. 2005; 115:1004–1007. [PubMed: 15805377]
32. Hajnal A, Smith GP, Norgren R. Oral sucrose stimulation increases accumbens dopamine in the rat. Am J Physiol Regul Integr Comp Physiol. 2004; 286:R31–7. [PubMed: 12933362]
33. Hammer RP Jr, Ricalde AA, Seatriz JV. Effects of opiates on brain development. Neurotoxicology. 1989; 10:475–483. [PubMed: 2696899]
34. Hoebel BG, Avena NM, Bocarsly ME, Rada P. Natural addiction: a behavioral and circuit model based on sugar addiction in rats. J Addict Med. 2009; 3:33–41. [PubMed: 21768998]
35. Holsti L, Grunau RE. Considerations for using sucrose to reduce procedural pain in preterm infants. Pediatrics. 2010; 125:1042–1047. [PubMed: 20403938]
36. Hu S, Sheng WS, Lokensgard JR, Peterson PK. Morphine induces apoptosis of human microglia and neurons. Neuropharmacology. 2002; 42:829–836. [PubMed: 12015209]
37. Jablonska B, Scafidi J, Aguirre A, Vaccarino F, Nguyen V, Borok E, Horvath TL, Rowitch DH, Gallo V. Oligodendrocyte regeneration after neonatal hypoxia requires FoxO1-mediated p27Kip1 expression. J Neurosci. 2012; 32:14775–14793. [PubMed: 23077062]
38. Johnston CC, Filion F, Snider L, Majnemer A, Limperopoulos C, Walker CD, Veilleux A, Pelausa E, Cake H, Stone S, Sherrard A, Boyer K. Routine sucrose analgesia during the first week of life in neonates younger than 31 weeks' postconceptional age. Pediatrics. 2002; 110:523–528. [PubMed: 12205254]
39. Juul SE, Beyer RP, Bammler TK, Farin FM, Gleason CA. Effects of neonatal stress and morphine on murine hippocampal gene expression. Pediatr Res. 2011; 69:285–292. [PubMed: 21178816]
40. Kehoe P, Blass EM. Behaviorally functional opioid systems in infant rats: II. Evidence for pharmacological, physiological, and psychological mediation of pain and stress. Behav Neurosci. 1986; 100:624–630. [PubMed: 3640642]
41. Knaepen L, Patijn J, van Kleef M, Mulder M, Tibboel D, Joosten EA. Neonatal repetitive needle pricking: plasticity of the spinal nociceptive circuit and extended postoperative pain in later life. Dev Neurobiol. 2013; 73:85–97. [PubMed: 22821778]
42. Lerch JP, Carroll JB, Spring S, Bertram LN, Schwab C, Hayden MR, Henkelman RM. Automated deformation analysis in the YAC128 Huntington disease mouse model. Neuroimage. 2008; 39:32–39. [PubMed: 17942324]

43. McKechnie L, Levene M. Procedural pain guidelines for the newborn in the United Kingdom. J Perinatol. 2008; 28:107–111. [PubMed: 17855806]
44. Nieman BJ, Flenniken AM, Adamson SL, Henkelman RM, Sled JG. Anatomical phenotyping in the brain and skull of a mutant mouse by magnetic resonance imaging and computed tomography. Physiol Genomics. 2006; 24:154–162. [PubMed: 16410543]
45. Nuseir KQ, Alzoubi KH, Alabwaini J, Khabour OF, Kassab MI. Sucrose-induced analgesia during early life modulates adulthood learning and memory formation. Physiol Behav. 2015; 145:84–90. [PubMed: 25846434]
46. Pomares FB, Funck T, Feier NA, Roy S, Daigle-Martel A, Ceko M, Narayanan S, Araujo D, Thiel A, Stikov N, Fitzcharles MA, Schweinhardt P. Histological Underpinnings of Grey Matter Changes in Fibromyalgia Investigated Using Multimodal Brain Imaging. J Neurosci. 2017; 37:1090–1101. [PubMed: 27986927]
47. Rada P, Avena NM, Hoebel BG. Daily bingeing on sugar repeatedly releases dopamine in the accumbens shell. Neuroscience. 2005; 134:737–744. [PubMed: 15987666]
48. Ranger M, Chau CM, Garg A, Woodward TS, Beg MF, Bjornson B, Poskitt K, Fitzpatrick K, Synnes AR, Miller SP, Grunau RE. Neonatal pain-related stress predicts cortical thickness at age 7 years in children born very preterm. PLoS One. 2013; 8:e76702. [PubMed: 24204657]
49. Ranger M, Zwicker JG, Chau CM, Park MT, Chakravarthy MM, Poskitt K, Miller SP, Bjornson BH, Tam EW, Chau V, Synnes AR, Grunau RE. Neonatal Pain and Infection Relate to Smaller Cerebellum in Very Preterm Children at School Age. J Pediatr. 2015; 167:292–298. e1. [PubMed: 25987534]
50. Rao R, Sampers JS, Kronsberg SS, Brown JV, Desai NS, Anand KJ. Neurobehavior of preterm infants at 36 weeks postconception as a function of morphine analgesia. Am J Perinatol. 2007; 24:511–517. [PubMed: 17907073]
51. Reboucas EC, Segato EN, Kishi R, Freitas RL, Savoldi M, Morato S, Coimbra NC. Effect of the blockade of mu1-opioid and 5HT2A-serotonergic/alpha1-noradrenergic receptors on sweet-substance-induced analgesia. Psychopharmacology (Berl). 2005; 179:349–355. [PubMed: 15821952]
52. Ren K, Blass EM, Zhou Q, Dubner R. Suckling and sucrose ingestion suppress persistent hyperalgesia and spinal Fos expression after forepaw inflammation in infant rats. Proc Natl Acad Sci U S A. 1997; 94:1471–1475. [PubMed: 9037077]
53. Ricalde AA, Hammer RP Jr. Perinatal opiate treatment delays growth of cortical dendrites. Neurosci Lett. 1990; 115:137–143. [PubMed: 2172870]
54. Roofthooft DW, Simons SH, Anand KJ, Tibboel D, van Dijk M. Eight Years Later, Are We Still Hurting Newborn Infants? Neonatology. 2014; 105:218–226. [PubMed: 24503902]
55. Salmaso N, Jablonska B, Scafidi J, Vaccarino FM, Gallo V. Neurobiology of premature brain injury. Nat Neurosci. 2014; 17:341–346. [PubMed: 24569830]
56. Sanchez ES, Bigbee JW, Fobbs W, Robinson SE, Sato-Bigbee C. Opioid addiction and pregnancy: perinatal exposure to buprenorphine affects myelination in the developing brain. Glia. 2008; 56:1017–1027. [PubMed: 18381654]
57. Seatriz JV, Hammer RP Jr. Effects of opiates on neuronal development in the rat cerebral cortex. Brain Res Bull. 1993; 30:523–527. [PubMed: 8384517]
58. Simons SH, van Dijk M, van Lingen RA, Roofthooft D, Duivenvoorden HJ, Jongeneel N, Bunkers C, Smink E, Anand KJ, van den Anker JN, Tibboel D. Routine morphine infusion in preterm newborns who received ventilatory support: a randomized controlled trial. JAMA. 2003; 290:2419–2427. [PubMed: 14612478]
59. Spangler R, Wittkowski KM, Goddard NL, Avena NM, Hoebel BG, Leibowitz SF. Opiate-like effects of sugar on gene expression in reward areas of the rat brain. Brain Res Mol Brain Res. 2004; 124:134–142. [PubMed: 15135221]
60. Spring S, Lerch JP, Henkelman RM. Sexual dimorphism revealed in the structure of the mouse brain using three-dimensional magnetic resonance imaging. Neuroimage. 2007; 35:1424–1433. [PubMed: 17408971]

61. Steadman PE, Ellegood J, Szulc KU, Turnbull DH, Joyner AL, Henkelman RM, Lerch JP. Genetic effects on cerebellar structure across mouse models of autism using a magnetic resonance imaging atlas. Autism Res. 2014; 7:124–137. [PubMed: 24151012]
62. Stevens B, Yamada J, Ohlsson A, Haliburton S, Shorkey A. Sucrose for analgesia in newborn infants undergoing painful procedures. Cochrane Database Syst Rev. 2016; 7:CD001069. [PubMed: 27420164]
63. Taddio A, Shah V, Shah P, Katz J. Beta-endorphin concentration after administration of sucrose in preterm infants. Arch Pediatr Adolesc Med. 2003; 157:1071–1074. [PubMed: 14609895]
64. Takane, Y. Constrained principal component analysis and related techniques. Boca Raton, FL: Chapman and Hall/CRC Press; 2014.
65. Tardif CL, Steele CJ, Lampe L, Bazin PL, Ragert P, Villringer A, Gauthier CJ. Investigation of the confounding effects of vasculature and metabolism on computational anatomy studies. Neuroimage. 2017; 149:233–243. [PubMed: 28159689]
66. Ullmann JF, Watson C, Janke AL, Kurniawan ND, Reutens DC. A segmentation protocol and MRI atlas of the C57BL/6J mouse neocortex. Neuroimage. 2013; 78:196–203. [PubMed: 23587687]
67. Vinall J, Miller S, Bjornson B, Fitzpatrick K, Poskitt K, Brant R, Synnes A, Cepeda I, Grunau R. Invasive procedures in preterm children: brain and cognitive development at school age. Pediatrics. 2014; 133:412–421. [PubMed: 24534406]
68. Walker CD. Nutritional aspects modulating brain development and the responses to stress in early neonatal life. Prog Neuropsychopharmacol Biol Psychiatry. 2005; 29:1249–1263. [PubMed: 16253410]
69. Walker CD, Xu Z, Rochford J, Johnston CC. Naturally occurring variations in maternal care modulate the effects of repeated neonatal pain on behavioral sensitivity to thermal pain in the adult offspring. Pain. 2008; 140:167–176. [PubMed: 18801618]
70. Zwicker JG, Grunau RE, Adams E, Chau V, Brant R, Poskitt KJ, Synnes A, Miller SP. Score for neonatal acute physiology-II and neonatal pain predict corticospinal tract development in premature newborns. Pediatr Neurol. 2013; 48:123–129. e1. [PubMed: 23337005]
71. Zwicker JG, Miller SP, Grunau RE, Chau V, Brant R, Studholme C, Liu M, Synnes A, Poskitt KJ, Stiver ML, Tam EW. Smaller Cerebellar Growth and Poorer Neurodevelopmental Outcomes in Very Preterm Infants Exposed to Neonatal Morphine. J Pediatr. 2016; 172:81–87. e2. [PubMed: 26763312]

A

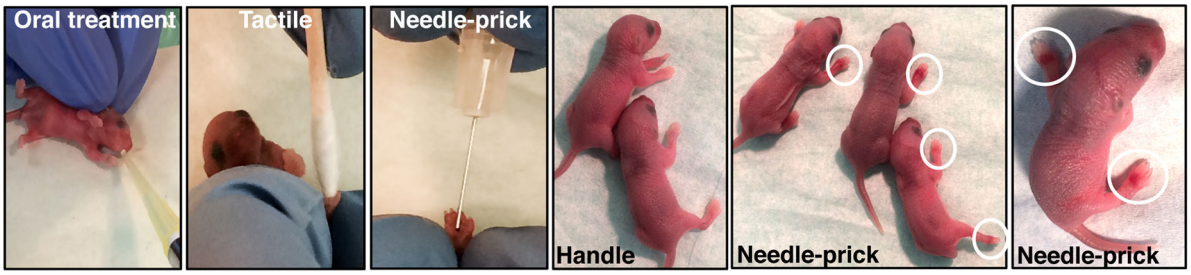

B

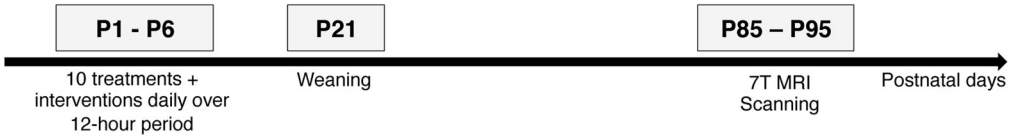

C

Treatment pre-intervention	Intervention	*Mean weight gain during treatment (P7 weight - P1 weight)*	*Mean body weight at MRI scan*	*n (%Males)*	*Survival rate*	Overall distribution (*N* = 109)
Water	Handle	2.2 ± 0.1 g	23.5 ± 0.8 g	18 (44,4%)	94,7%	*N*= 52
Water	Tactile	2.1 ± 0.1 g	23.7 ± 0.9 g	16 (56,2%)	90,5%	
Water	Needle-prick	2.0 ± 0.1 g	23.5 ± 1.0 g	18 (50,0%)	95,0%	
Sucrose 24%	Handle	1.7 ± 0.1 g	22.7 ± 0.7 g	17 (41,2%)	94,7%	*N* = 57
Sucrose 24%	Tactile	1.9 ± 0.1 g	22.7 ± 0.8 g	22 (45,4%)	95,8%	
Sucrose 24%	Needle-prick	1.9 ± 0.1 g	22.9 ± 0.9 g	18 (38,9%)	100,0%	

Figure 1. Neonatal mouse model of repetitive sucrose exposure given for procedural pain

(A) Representative images showing C57Bl/6J mouse pups receiving oral sucrose treatment preceding 10 interventions daily: Handle, Tactile or Needle-prick. Ecchymosis and inflamed paws are highlighted by white circles showing focal needle-prick intervention effects. **(B)** Experimental protocol illustrating treatment/intervention timeline. Brain tissue was collected between P85–P95 for 7T MRI scanning. **(C)** Neonatal mice (n = 109) were assigned randomly across treatment/intervention groups (total of 6 groups). Distribution, mean weight gain over treatment period, mean body weight at MRI scan, sex ratio and survival amongst groups during the current study are provided.

A

Brain structure	Volume (mean ± SD) absolute (mm³)		Effect of treatment	
	Vehicle	Sucrose 24%	*P*-value	FDR
Cerebrum / Cerebral cortex				
Cingulate Cortex area 25	0.491 ± 0.019	0.477 ± 0.022	<0.0001	3%
Caudomedial entorhinal cortex	5.30 ± 0.21	5.18 ± 0.23	0.0007	4%
Primary visual cortex	2.07 ± 0.10	2.00 ± 0.14	0.0001	3%
Primary visual cortex binocular area	2.086 ± 0.091	2.025 ± 0.131	0.0007	4%
Hippocampus	19.79 ± 0.66	19.30 ± 0.89	0.0001	3%
Dentate gyrus of hippocampus	3.70 ± 0.14	3.60 ± 0.20	0.0003	4%
Stratum granulosum hippocampus	0.976 ±0.035	0.950 ±0.054	0.0002	4%
Pre-para subiculum	2.003 ± 0.081	1.942 ± 0.128	0.0003	4%
Cerebrum / Cerebral Nuclei				
Lateral septum	3.16 ± 0.15	3.08 ± 0.14	0.0005	4%
Cerebellum				
Lobule 3: central lobule (dorsal)	2.04 ± 0.11	1.97 ± 0.12	0.0001	4%
Crus 1: ansiform lobule (lobule 6)	4.29 ± 0.18	4.18 ± 0.21	0.0005	4%
Lobule 3 white matter	0.227 ± 0.012	0.220 ± 0.014	0.0004	4%
Lobule 4-5 white matter	0.618 ± 0.027	0.601 ± 0.032	0.0002	4%
Simple lobule white matter	0.439 ± 0.021	0.426 ± 0.025	0.0006	4%
Crus 1 white matter	0.406 ± 0.021	0.392 ± 0.023	0.0001	3%
Paraflocculus white matter	0.308 ± 0.017	0.296 ± 0.016	<0.0001	3%
Ventricular system				
Lateral ventricle	3.79 ± 0.29	3.62 ± 0.24	0.0001	3%
Fiber tracts				
Corpus callosum	13.02 ± 0.53	12.61 ± 0.72	0.0001	3%
Fimbriae	3.50 ± 0.18	3.35 ± 0.20	<0.0001	1%
Fornix	0.649 ± 0.027	0.633 ± 0.031	0.0005	4%
Stria terminalis	0.918 ± 0.042	0.887 ± 0.055	0.0001	3%

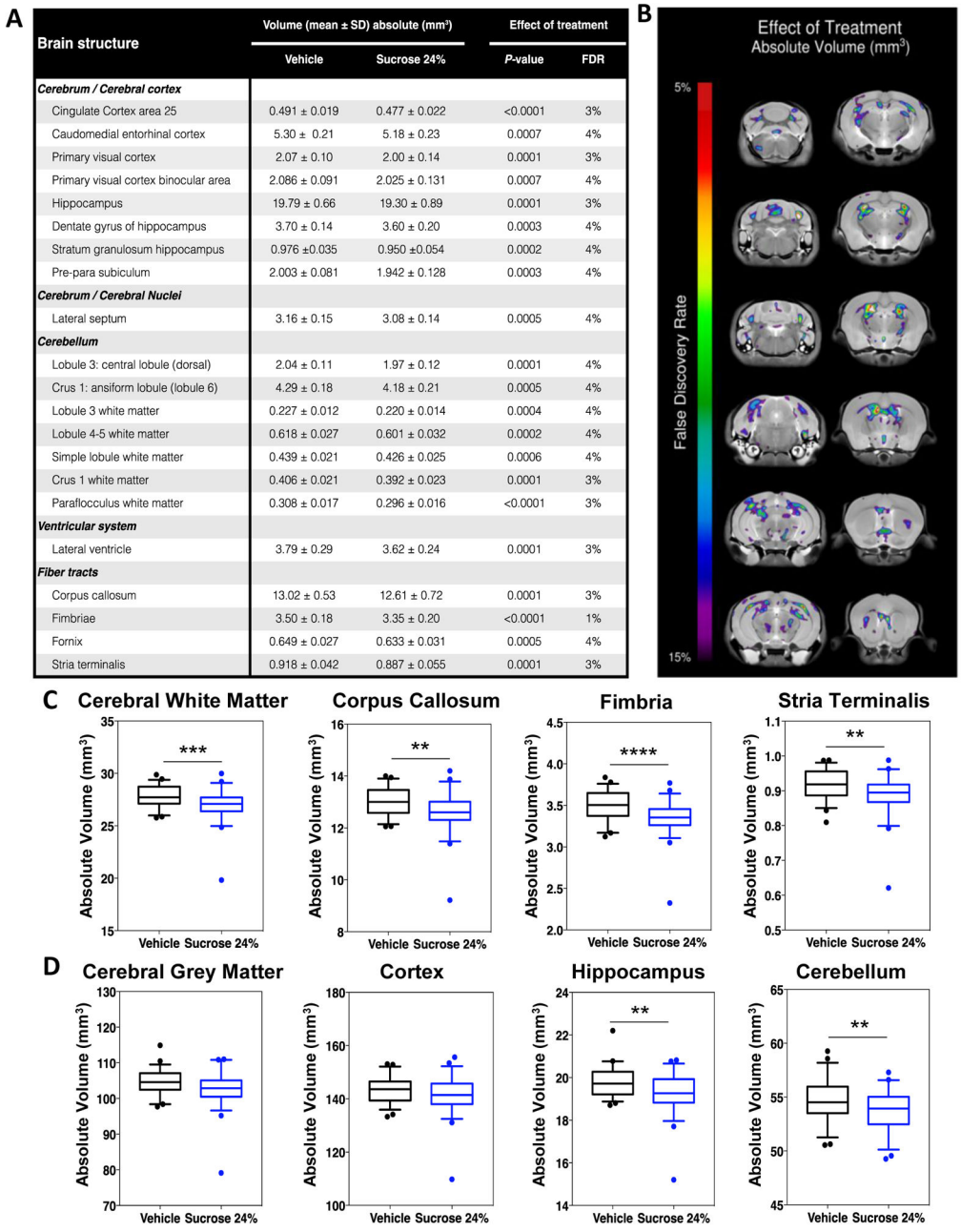

Figure 2. Widespread smaller volumes in 21 brain regions at adulthood in mice exposed to neonatal repetitive sucrose irrespective of intervention

(A) List of the 21 brain regions, including cortical, subcortical, cerebellar structures and fiber tracts, that were significantly smaller (FDR < 5%) at adulthood. **(B)** Sample of coronal slices showing cross-regional voxel-wise differences of absolute brain regional volumes between mice exposed to repetitive Vehicle compared to Sucrose, irrespective of intervention. FDR 5–15% are shown. **(C)** Box-plot figures of brain volumes comparing mice in Vehicle versus Sucrose groups in white matter (FDR = 3%), corpus callosum (FDR = 3%), fimbria (FDR = 3%) and stria terminalis (FDR = 1%). **(D)** Box-plot figures of brain volumes comparing mice in Vehicle versus Sucrose groups in grey matter (FDR = 6%),

cortex (FDR = 17%), hippocampus (FDR = 3%) and cerebellum (FDR = 4%). $n = 52–57$ per group. $^{**}P < 0.01$, $^{***}P < 0.001$, $^{***}P < 0.0001$; FDR, false discovery rate.

Table 1

Component loadings for treatment in CPCA modeling

Factors	PC1		PC2	
	Loading	P-value	Loading	P-value
Total brain volume	0.746	0,0000	0.611	0.0000
Sex	0.623	0,0000	−0.762	0.0000
Vehicle vs Sucrose	−0.037	0.7005	**−0.360**	**0.0001**

CPCA factor loadings for Vehicle versus Sucrose model; two principal components (PC)s were extracted from the predicted solution, where PC1 reflected total brain volume and sex and PC2 reflected treatment; explained variance for PC1 and PC2 are 26.2%, 22.7% respectively, $n = 52–57$ per group. Significant loadings (Bonferroni $P < 0.013$) particular to treatment shown in **bold**.

CPCA, constrained principal component analysis.

Table 2

Regional brain volumes variance explained by treatment (Vehicle vs Sucrose) in CPCA modeling.

Brain Structure	PC1		PC2	
	Loading	P-value	Loading	P-value
Cerebrum / Cerebral cortex	0.279	0.0021	**0.820**	**0.0000**
Amygdalo piriform transition area	0.255	0.0004	**0.685**	**0.0000**
Caudo medial entorhinal cortex	0.297	0.0070	**0.665**	**0.0000**
Postero lateral cortical amygdaloid area	0.312	0.0013	**0.554**	**0.0000**
Postero medial cortical amygdaloid area	0.225	0.0017	**0.748**	**0.0000**
Rostral amygdalo piriform area	0.271	0.0092	**0.525**	**0.0000**
Ventral tenia tecta	0.191	0.0292	**0.399**	**0.0000**
Cerebrum / Cerebral nuclei				
Bed nucleus of stria terminalis	0.279	0.0021	**0.820**	**0.0000**
Brainstem				
Medulla	0.203	0.0094	**0.351**	**0.0002**
Superior olivary complex	0.061	0.4517	**0.370**	**0.0001**
Cerebellum				
Lobules 4–5: culmen (ventral and dorsal)	0.329	0.0004	**0.536**	**0.0000**
Lobule 7: tuber (or folium)	0.185	0.0129	**0.418**	**0.0000**
Lobule 8: pyramis	0.190	0.0233	**0.439**	**0.0000**
Copula pyramis lobule 8	0.271	0.0020	**0.427**	**0.0000**
Trunk of lobules 6–8 white matter	0.265	0.0009	**0.391**	**0.0000**
Lobule 8 white matter	0.110	0.1854	**0.394**	**0.0001**
Lobule 9: uvula	0.266	0.0006	**0.507**	**0.0000**
Lobule 9 white matter	0.201	0.0106	**0.484**	**0.0000**
Lobule 10: nodulus	0.260	0.0015	**0.433**	**0.0000**
Flocculus FL	0.156	0.0549	**0.509**	**0.0000**
Flocculus white matter	0.099	0.2381	**0.397**	**0.0000**
Paraflocculus PFL	0.250	0.0019	**0.329**	**0.0002**
Ventricular system				
Third ventricle	0.410	0.0010	**0.483**	**0.0001**

CPCA factor loadings for analysis of treatment effect on regional brain volumes. Component loadings for PC1 and PC2 and their *P*-values for the 22 brain regions that passed the Bonferroni cut-off ($P < 0.013$) are listed. Treatment (represented in PC2) loaded uniquely on 22 brain regions, reflecting that mice exposed to Sucrose have significantly smaller volumes in these specific brain areas compared to Vehicle ($P < 0.013$), n per group 52–57.

CPCA, constrained principal component analysis; PC, principal component.

Table 3

Component loadings for intervention split by treatment – Vehicle.

Factors	PC1		PC2		PC3	
	Loading	*P*-value	Loading	*P*-value	Loading	*P*-value
Total brain volume	0.678	0.0000	0.693	0.0000	0.242	0.0812
Sex	0.679	0.0000	−0.602	0.0000	−0.420	0.0026
Needle-prick intervention	−0.035	0.8044	−0.067	0.6315	0.079	0.5723
Tactile intervention	−0.173	0.2238	**0.469**	**0.0014**	**−0.771**	**0.0000**

Split analysis by treatment (Vehicle) CPCA factor loadings for Vehicle groups model; three PCs were extracted from the predicted solution, where PC1 reflected total brain volume and sex, PC2 Tactile intervention, and PC3 sex and Tactile intervention; explained variance for PC1, PC2, PC3 are 22%, 15.3%, and 6.3% respectively. Vehicle/Handle ($n = 18$), Vehicle/Tactile ($n = 16$), or Vehicle/Needle-prick ($n = 18$). Significant loadings (Bonferroni $P < 0.013$) particular to intervention shown in **bold**.

CPCA, constrained principal component analysis; PC, principal component.

Table 4

Effects of exposure to interventions on adult mice regional brain volumes within the 3 groups: CPCA analysis split by treatment - Vehicle.

Brain Structure	PC1		PC2		PC3	
	Loading	*P*-value	Loading	*P*-value	Loading	*P*-value
Cerebrum						
Cerebral cortex/cortical plate						
Cingulate cortex area 30	−0.572	**0.0000**	0.398	**0.0000**	−0.359	0.0004
Secondary auditory cortex dorsal area	−0.594	**0.0000**	0.386	**0.0002**	−0.331	0.0005
Caudomedial entorhinal cortex	−0.096	0.3225	0.510	**0.0001**	−0.376	0.0006
Cingulum	−0.566	**0.0000**	0.358	**0.0001**	−0.291	0.0010
Ectorhinal cortex	−0.608	**0.0000**	0.446	**0.0000**	−0.311	0.0147
Postero lateral cortical amygdaloid area	−0.330	0.0050	0.488	**0.0000**	−0.318	0.0216
Perirhinal cortex	−0.525	**0.0000**	0.410	**0.0000**	−0.319	0.0054
Rostral amygdalo piriform area	−0.169	0.1585	0.548	**0.0000**	−0.300	0.0072
Temporal association area	−0.540	**0.0000**	0.400	**0.0002**	−0.271	0.0361
Primary visual cortex	−0.519	**0.0000**	0.490	**0.0000**	−0.333	0.0010
Secondary visual cortex lateral area	−0.625	**0.0000**	0.425	**0.0000**	−0.332	0.0006
Hippocampus	−0.433	**0.0001**	0.670	**0.0000**	−0.351	0.0004
Dentate gyrus of hippocampus	−0.241	0.0875	0.602	**0.0000**	−0.264	0.0259
Stratum granulosum of hippocampus	−0.318	0.0191	0.587	**0.0000**	−0.241	0.0507
Cerebral nuclei						
Lateral septum	−0.671	**0.0000**	0.372	**0.0000**	−0.287	0.0065
Medial septum	−0.547	**0.0000**	0.487	**0.0001**	−0.230	0.0481
Nucleus accumbens	−0.669	**0.0000**	0.405	**0.0000**	−0.252	0.0055
Brainstem						
Midbrain	−0.538	**0.0000**	0.518	**0.0000**	−0.243	0.0286
Cerebellum						
Cerebellar cortex/vermis						
Lobule 3 central lobule dorsal	−0.260	0.0048	0.540	**0.0001**	−0.215	0.0987
Lobule 3 white matter	−0.285	0.0027	0.483	**0.0001**	−0.292	0.0308
Lobules 4–5 culmen ventral and dorsal	−0.161	0.2575	0.493	**0.0002**	−0.163	0.2286

Brain Structure	PC1		PC2		PC3	
	Loading	*P*-value	Loading	*P*-value	Loading	*P*-value
Lobule 7 tuberor folium	−0.083	0.4901	0.528	**0.0000**	−0.043	0.7456
Lobule 8 pyramis	−0.221	0.0430	0.517	**0.0002**	−0.006	0.9641
Lobule 9 uvula	−0.285	0.0065	0.566	**0.0001**	−0.122	0.3305
Cerebellar cortex/hemispheres						
Simple lobule 6	−0.533	**0.0000**	0.484	**0.0000**	−0.121	0.3051
Crus 1 white matter	−0.478	**0.0000**	0.525	**0.0000**	−0.304	0.0005
Crus 2 ansiform lobule 7	−0.479	**0.0000**	0.530	**0.0000**	−0.185	0.0301
Crus 2 white matter	−0.541	**0.0000**	0.448	**0.0000**	−0.267	0.0033
Paramedian lobule 7	−0.471	**0.0000**	0.503	**0.0002**	−0.056	0.6141
Trunk of crus 2 and paramedian white matter	−0.532	**0.0000**	0.404	**0.0002**	−0.192	0.0482
Flocculus FL	−0.120	0.2667	0.592	**0.0000**	−0.077	0.5402
Fiber Tracts						
Cranial nerves						
Lateral olfactory tract	−0.440	**0.0000**	0.385	**0.0002**	−0.413	0.0047
Medial lemniscus medial longitudinal fasciculus	−0.338	0.0006	0.536	**0.0002**	−0.172	0.1684
Lateral forebrain bundle system						
Corticospinal tract pyramids	−0.197	0.0567	0.493	**0.0002**	0.038	0.7919
Extrapyramidal fiber system						
Ventral tegmental decussation	−0.506	**0.0000**	0.609	**0.0000**	−0.184	0.0607
Medial forebrain bundle system						
Fimbria	−0.552	**0.0000**	0.360	**0.0001**	−0.160	0.1743
Fornix	−0.565	**0.0000**	0.454	**0.0000**	−0.272	0.0133
Fasciculus retroflexus	−0.645	**0.0000**	0.325	**0.0000**	−0.152	0.1625
Stria medullaris	−0.665	**0.0000**	0.338	**0.0002**	−0.087	0.4835
Other						
Pre-para subiculum	−0.249	0.0171	0.495	**0.0002**	−0.371	0.0077

Component loadings for PC1, PC2 and PC3 and their *P*-values for the 40 brain regions that passed the Bonferroni cut-off ($P < 0.013$; shown in **bold** font) for significance are listed; $n = 16–18$ per group. Brain regions are presented by anatomical distribution according to Allen Mouse Brain Atlas.

Significant P-values CPCA, constrained principal component analysis; PC, principal component.

Table 5

Component loadings for intervention split by treatment – Sucrose.

Factors	PC1		PC2		PC3	
	Loading	*P*-value	Loading	*P*-value	Loading	*P*-value
Total brain volume	0.723	0.0000	0.563	0.0000	0.392	0.0025
Sex	0.404	0.0015	−0.833	0.0000	0.367	0.0067
Needle-prick intervention	**−0.469**	**0.0005**	0.108	0.4286	**0.787**	**0.0000**
Tactile intervention	**0.428**	**0.0014**	0.020	0.8743	**−0.708**	**0.0000**

CPCA, constrained principal component analysis; PC, principal component.

Table 6

Effects of exposure to interventions on adult mice regional brain volumes within the 3 groups: CPCA analysis split by treatment - Sucrose.

Brain Structure	PC1		PC2		PC3	
	Loading	*P*-value	Loading	*P*-value	Loading	*P*-value
Cerebrum						
Cerebral cortex/cortical plate						
Cingulate cortex area 24a	0.736	**0.0000**	0.409	0.0005	0.187	0.0150
Cingulate cortex area 24b	0.636	**0.0001**	0.283	0.0232	0.187	0.0753
Cingulate cortex area 24bapos	0.685	**0.0002**	0.336	0.0143	0.115	0.2838
Cingulate cortex area 25	0.717	**0.0000**	0.348	**0.0002**	0.053	0.5945
Cingulate cortex area 29b	0.707	**0.0000**	0.443	0.0008	0.163	0.0927
Cingulate cortex area 30	0.811	**0.0000**	0.446	0.0017	0.161	0.0586
Cingulate cortex area 32	0.742	**0.0000**	0.125	0.3233	0.246	0.0030
Amygdalo piriform transition area	0.398	**0.0002**	0.643	**0.0000**	0.157	0.1007
Primary auditory cortex	0.715	**0.0000**	0.483	**0.0000**	0.236	0.0016
Secondary auditory cortex dorsal area	0.707	**0.0000**	0.499	**0.0000**	0.261	0.0015
Secondary auditory cortex ventral area	0.683	**0.0001**	0.474	**0.0002**	0.151	0.0649
Cingulum	0.759	**0.0000**	0.417	0.0015	0.211	0.0059
Dorsal intermediate entorhinal cortex	0.550	**0.0000**	0.528	**0.0000**	0.220	0.0074
Dorsolateral entorhinal cortex	0.569	**0.0001**	0.426	0.0009	0.278	0.0035
Dorsolateral orbital cortex	0.585	**0.0000**	0.041	0.7359	0.264	0.0043
Dorsal teniatecta	0.651	**0.0000**	0.304	0.0030	0.032	0.7966
Ectorhinal cortex	0.762	**0.0000**	0.402	**0.0002**	0.250	0.0016
Frontal cortex area 3	0.712	**0.0002**	0.259	0.0751	0.211	0.0078
Insular region not subdivided	0.691	**0.0000**	0.335	**0.0002**	0.105	0.2131
Lateral orbital cortex	0.761	**0.0000**	0.032	0.7989	0.219	0.0167
Lateral parietal association cortex	0.641	**0.0000**	0.452	**0.0000**	0.209	0.0453
Primary motor cortex	0.694	**0.0001**	0.371	0.0039	0.236	0.0053
Secondary motor cortex	0.695	**0.0001**	0.342	0.0060	0.178	0.0464
Medial entorhinal cortex	0.489	**0.0001**	0.466	**0.0000**	0.208	0.0330
Medial orbital cortex	0.731	**0.0000**	−0.029	0.8023	0.254	0.0137

Brain Structure	PC1		PC2		PC3	
	Loading	*P*-value	Loading	*P*-value	Loading	*P*-value
Medial parietal association cortex	0.679	**0.0000**	0.439	**0.0001**	0.216	0.0313
Piriform cortex	0.679	**0.0000**	0.467	**0.0000**	0.119	0.1831
Perirhinal cortex	0.704	**0.0000**	0.447	**0.0001**	0.284	0.0008
Parietal cortex posterior area rostral part	0.634	**0.0000**	0.432	**0.0002**	0.203	0.0658
Primary somatosensory cortex	0.761	**0.0000**	0.300	0.0274	0.234	0.0006
Primary somatosensory cortex barrel field	0.774	**0.0000**	0.412	0.0004	0.254	0.0007
Primary somatosensory cortex dysgranular	0.711	**0.0000**	0.389	0.0011	0.264	0.0006
Primary somatosensory cortex forelimb	0.711	**0.0000**	0.407	0.0005	0.256	0.0016
Primary somatosensory cortex hindlimb	0.660	**0.0000**	0.431	**0.0000**	0.254	0.0087
Primary somatosensory cortex shoulder	0.660	**0.0000**	0.438	**0.0001**	0.248	0.0142
Primary somatosensory cortex trunk	0.627	**0.0000**	0.458	**0.0000**	0.224	0.0354
Primary somatosensory cortex upper lip	0.762	**0.0000**	0.344	0.0046	0.214	0.0030
Secondary somatosensory cortex	0.738	**0.0000**	0.306	0.0015	0.140	0.1075
Temporal association area	0.736	**0.0000**	0.389	0.0008	0.205	0.0195
Primary visual cortex	0.675	**0.0000**	0.428	**0.0000**	0.216	0.0236
Primary visual cortex binocular area	0.719	**0.0000**	0.487	**0.0000**	0.233	0.0086
Primary visual cortex monocular area	0.710	**0.0000**	0.482	**0.0001**	0.203	0.0342
Secondary visual cortex lateral area	0.743	**0.0000**	0.419	**0.0000**	0.256	0.0015
Secondary visual cortex mediolateral area	0.688	**0.0000**	0.480	**0.0001**	0.220	0.0304
Secondary visual cortex mediomedial area	0.666	**0.0000**	0.541	**0.0000**	0.193	0.0343
Claustrum ventral part	0.689	**0.0000**	0.370	**0.0003**	0.084	0.3957
Ventral intermediate entorhinal cortex	0.462	**0.0000**	0.551	**0.0000**	0.192	0.0208
Ventral orbital cortex	0.802	**0.0000**	0.140	0.2341	0.187	0.0445
Olfactory bulbs	0.496	**0.0000**	0.677	**0.0000**	−0.065	0.4716
Hippocampus	0.687	**0.0001**	0.667	**0.0000**	0.169	0.0056
Dentate gyrus of hippocampus	0.631	**0.0002**	0.648	**0.0000**	0.147	0.0876
Stratum granulosum of hippocampus	0.640	**0.0001**	0.626	**0.0000**	0.159	0.0738
Cerebral cortex/subcortical plate						
Claustrum	0.737	**0.0000**	0.175	0.1660	0.307	0.0007
Claustrum dorsal part	0.683	**0.0000**	0.397	**0.0000**	0.139	0.1337

Pain. Author manuscript; available in PMC 2018 August 01.

Brain Structure	PC1		PC2		PC3	
	Loading	*P*-value	Loading	*P*-value	Loading	*P*-value
Dorsal nucleus of the endopiriform	0.762	**0.0000**	0.300	0.0092	0.130	0.1300
Intermediate nucleus of the endopiriform claustrum	0.736	**0.0000**	0.249	0.0356	0.187	0.0248
Ventral nucleus endopiriform claustrum	0.636	**0.0001**	0.490	**0.0000**	0.133	0.1561
Amygdala	0.613	**0.0000**	0.648	**0.0000**	0.087	0.3122
Cerebral nuclei						
Fundus of striatum	0.737	**0.0000**	0.374	0.0030	0.102	0.2240
Nucleus accumbens	0.795	**0.0000**	0.343	0.0044	0.215	0.0020
Globus pallidus	0.785	**0.0000**	0.398	0.0027	0.166	0.0272
Lateral septum	0.682	**0.0000**	0.457	**0.0000**	0.225	0.0074
Medial septum	0.682	**0.0000**	0.478	**0.0000**	0.106	0.3023
Olfactory tubercle	0.572	**0.0002**	0.464	**0.0001**	0.019	0.8555
Basal forebrain	0.716	**0.0000**	0.565	**0.0000**	0.137	0.0676
Brainstem						
Interbrain						
Thalamus	0.845	**0.0002**	0.369	0.0188	0.216	0.0081
Hypothalamus	0.639	**0.0001**	0.671	**0.0000**	0.099	0.2161
Midbrain						
Midbrain	0.788	**0.0000**	0.474	**0.0000**	0.195	0.0020
Colliculus inferior	0.687	**0.0000**	0.460	**0.0000**	0.171	0.0428
Colliculus superior	0.764	**0.0000**	0.507	**0.0000**	0.117	0.1248
Periaqueductal grey	0.757	**0.0000**	0.369	**0.0001**	0.245	0.0012
Interpedunclar nucleus	0.533	**0.0000**	0.396	0.0007	0.171	0.1388
Hindbrain						
Pons	0.502	**0.0000**	0.409	**0.0000**	0.178	0.1237
Cerebellum						
Cerebellar cortex/vermis						
Lobule 3 central lobule dorsal	0.507	**0.0001**	0.297	0.0018	0.244	0.1156
Lobules 4–5 culmen ventral and dorsal	0.401	**0.0001**	0.443	**0.0000**	0.215	0.1028
Lobule 3 white matter	0.529	**0.0001**	0.242	0.0136	0.212	0.1491
Lobules 4–5 white matter	0.529	**0.0000**	0.319	0.0058	0.109	0.3825

Brain Structure	PC1		PC2		PC3	
	Loading	*P*-value	Loading	*P*-value	Loading	*P*-value
Cerebellar cortex/hemispheres						
Crus 1 ansiform lobule 6	0.406	**0.0000**	0.535	**0.0000**	0.248	0.0021
Simple lobule white matter	0.554	**0.0000**	0.297	0.0012	0.350	0.0027
Crus1 white matter	0.515	**0.0000**	0.464	**0.0000**	0.287	0.0007
Trunk of simple and crus1 white matter	0.430	**0.0000**	0.407	**0.0001**	0.321	0.0021
Simple lobule 6	0.557	**0.0000**	0.375	**0.0000**	0.378	0.0010
Cerebellar nuclei						
Dentate nucleus	0.612	**0.0000**	0.277	0.0031	0.348	0.0063
Nucleus interpositus	0.541	**0.0000**	0.457	**0.0000**	0.300	0.0021
Fastigial nucleus	0.494	**0.0000**	0.346	0.0011	0.315	0.0031
Fiber Tracts						
Cranial nerves						
Lateral olfactory tract	0.573	**0.0000**	0.403	**0.0001**	0.074	0.4702
Cerebellum related fiber tracts						
Cerebellar peduncle superior	0.716	**0.0000**	0.344	**0.0000**	0.229	0.0117
Lateral forebrain bundle system						
Internal capsule	0.765	**0.0001**	0.511	**0.0002**	0.233	0.0005
Extrapyramidal fiber system						
Ventral tegmental decussation	0.696	**0.0000**	0.462	**0.0001**	0.204	0.0039
Medial forebrain bundle system						
Anterior commissure pars anterior	0.659	**0.0002**	0.613	**0.0000**	0.194	0.0273
Anterior commissure pars posterior	0.695	**0.0000**	0.446	**0.0001**	0.210	0.0196
Fasciculus retroflexus	0.778	**0.0002**	0.396	0.0058	0.244	0.0037
Ventricular System						
Ventricular System						
Subependymale zone rhinocele	0.458	**0.0003**	0.694	**0.0000**	0.067	0.4747
Cerebral aqueduct	0.644	**0.0000**	0.172	0.1101	0.130	0.2843
Other						
Pre-para subiculum	0.663	**0.0001**	0.537	**0.0000**	0.162	0.0651

Pain. Author manuscript; available in PMC 2018 August 01.

Component loadings for PC1, PC2 and PC3 and their *P*-values for the 95 brain regions that passed the Bonferroni cut-off ($P < 0.013$; shown in **bold** font) for significance are listed; $n = 17–22$ per group. Brain regions are presented by anatomical distribution according to Allen Mouse Brain Atlas.

CPCA, constrained principal component analysis; PC, principal component.